IEEE Access
Multidisciplinary | Rapid Review | Open Access Journal

Received 22 November 2022, accepted 2 January 2023, date of publication 13 January 2023, date of current version 19 January 2023.

Digital Object Identifier 10.1109/ACCESS.2023.3236665

RESEARCH ARTICLE

Development of an Adaptive Linear Mixture Model for Decomposition of Mixed Pixels to Improve Crop Area Estimation Using Artificial Neural Network

ARUN KANT DWIVEDI[1], ARUN KUMAR SINGH[2], (Member, IEEE), DHARMENDRA SINGH[2], (Senior Member, IEEE), AND HARISH KUMAR[3]

[1]Department of Computer Science and Engineering, IIT Roorkee, Roorkee 247667, India
[2]Department of Electronics and Communication Engineering, IIT Roorkee, Roorkee 247667, India
[3]Department of Computer Science, College of Computer Science, King Khalid University, Abha 61413, Saudi Arabia

Corresponding author: Dharmendra Singh (dharm@ec.iitr.ac.in)

This work was supported in part by the Drone Research Centre, IIT Roorkee; and in part by the Deanship of Scientific Research at King Khalid University, Abha, Saudi Arabia, under Grant R.G.P. 2/198/43.

ABSTRACT Precise spatial information of crop distribution is vital for government and research organizations to monitor agriculture activities like crop health monitoring, crop yield prediction, and food security. Mapping of crop area is challenging in smallholder farming like India, where crop parcels are smaller than two hectares. With an extension of artificial intelligence, an artificial neural network has ability to learn the spectral feature of multispectral satellite images and map them to a land cover class. However, mixed pixel is a challenging problem in pixel wise classification of coarse resolution satellite images. The linear mixture model is successfully utilized to unmix the signals of a mixed classes. The success of linear mixture model is depending on the selection of endmembers of a mixed class. Therefore, this paper presents an adaptive approach for automatic selection of endmembers of a mixed pixel in linear mixture model using spectral and spatial information. The proposed approach is capable of extracting the fraction area cover of each class by using a constrained least-squares error solution. The GPS field surveys, and drone images are employed to create reference data for the accuracy assessment of proposed algorithm. The experimentation results indicate that the solution of the proposed approach outperformed recent baseline methods in terms of efficiency and accuracy of pixelwise estimated area and overall estimated area of various land cover classes.

INDEX TERMS Smallholder farming, area estimation, artificial neural network, linear mixture model, mixed pixels, precision agriculture monitoring.

I. INTRODUCTION

Sustainable agriculture information system is important for agricultural activities by providing services like crop area estimation which helps in precise utilization of agricultural inputs like fertilizers and pesticide. It also helps to maximize productivity per drop of water which is a scarce resource these days [1]. Crop area estimation and crop yield prediction in advance of harvesting ensures the smooth market management and food security [2]. Precision agriculture is an important weapon against poverty and hunger and consistently making life better for billions of people across the globe. In recent time, agriculture is facing stiff challenges in the form of climate change, global warming, soil erosion, desertification, shrinking landholdings, crop failures etc. Agriculture information system (AIS) employs modern technologies like information and communication technology [3], wireless sensors [4], internet of things [5], satellite data [6], and drone images [7] become vital to keep agriculture sustainable, viable, smart and adaptive

The associate editor coordinating the review of this manuscript and approving it for publication was Vivek Kumar Sehgal.

to future challenges. A traditional agriculture information system uses global positioning system (GPS) for accurate mapping of agricultural fields [8]. Another cost optimized solution - Differential Global Positioning System (DGPS) uses localized data for robot guidance [9]. UAVs although provide high resolution data required for smart agriculture but cost and ease of controlling them are major roadblocks in their widespread use [10], [11]. Similarly, IoT provides live tracking of vital parameters like temperature, humidity, and soil moisture, but installation and maintenance of sensors for this is unviable especially for small landholders practicing subsistence farming [12]. In developing countries like India, the average size of operational holdings has decreased to 1.08 hectares according to latest Agriculture Census [13]. Amongst these around 86.2% farmers are marginal cultivating less than one-hectare land. This situation results in low upfront investment in agriculture modernization as there is no economies of scale. Thus, AIS technologies mentioned above apart from satellite imagery are unaffordable for this large farming community [14]. Satellite image processing techniques are also important component of AIS to identify, analyze, and manage diverse crop fields. In [15] the author reviews how interpreting satellite images for key aspects of farming like water stress, time and quantity of farm inputs, crop diseases and accessing yield quality is less tedious, economical and efficient compared to expert recommendation or physical laboratory testing. Satellite images are most popular source that is suitable for providing land cover information which is economical and feasible [16].

Satellite data predominately used for land cover mapping due to its high temporal data acquisition and wide spatial coverage [17]. Nowadays, several earth observation satellites have been launched with numerous spatial, spectral, and temporal resolutions [18]. These freely available satellite imageries are widely used in crop type classification [19]. Due to the limitation of optical imagery in adverse weather condition, Synthetic Aperture Radar (SAR) imagery is used in differentiating multiple land cover classes [20], [21]. With generous resource of satellite imagery and artificial intelligence techniques provide a major enhancement in satellite image classification [22], [23]. Area estimation of agriculture land for precision agriculture monitoring is done using various machine learning algorithms [24]. Crop type identification using object based classification and decision tree (DT) algorithm is done by using texture and spatial feature of satellite images [25]. Agriculture crop like rice, sugarcane, and cotton are classified using spectral signature library created by space borne hyperspectral data [26]. Satellite imagery is used for estimating fractional vegetation cover, shrub lands and grasslands in arid and semiarid areas for desertification monitoring [27], [28]. Apart from these, satellite images also find application in intra class classification using drone and satellite data fusion [29]. For precision crop monitoring, sparse and dense sugarcane crop areas are segregated in Landsat 8 imagery using adaptive thresholding method [30]. In small landholding, mixed pixels are the major problem in classification of coarse resolution satellite imagery [31], [32]. These mixed pixels are present on boundary of land cover classes, and contain more than one land cover class. Therefore, in order to improve the accuracy of the land cover classification, there is a need for decomposition of these mixed pixels.

An artificial neural network (ANN) is widely employed to classify satellite images in various land cover classes [33], [34]. In [35], an adaptive neuro-fuzzy (ANF) algorithm is developed for mixed pixel decomposition, wherein exponential normalized output of neural network is used as a membership criterion of each class for a mixed pixel. But exponential normalized output of neural network is not exact same as fractional values of all membership classes of mixed pixel. Similarly, spectral mixture analysis (SMA) techniques are widely employed for sub-pixel analysis of mixed land cover classes [36]. In linear mixture model (LMM), the reflected radiation from mixed land surface is the linear combination of reflected radiation of its endmember classes [37]. However, the limitation of LMM is that it cannot give solution when number of unknowns (endmembers of mixed pixel) are greater than the number of equations (spectral bands) [38], [39]. Moreover, linear mixture model also requires spectral variability of endmember spectra [40], [41]. Too many endmembers and spectrally similar endmembers leads to error in fractional distribution among endmembers [42], [43]. Accordingly, the success of linear mixture model is depending on the selection of endmembers [44].

Recognizing this paradox, the objective of this paper is to develop an adaptive method for selecting endmembers in linear mixture model and the aim of proposed method is to estimate the crop area that is more accurate and more optimal compared to alternate methods that have been carried out with a similar cost. The major contributions of proposed work are summarized as follows: firstly, several supervised classification algorithms were explored to classify satellite images in various crop classes, and it was observed that artificial neural network performed well. Secondly the output of artificial neural network is used as a spatial constraint for mixed pixel extraction. Mixed pixels and pure pixels are extracted from Satellite images in order to decompose them to improve accuracy of crop area estimation. Thirdly, the proposed adaptive linear mixture model is employed for decomposition of mixed pixel into relevant classes using least square error solution. The performance of the proposed adaptive linear mixture model is evaluated with various performance metrics and comprehensive comparison were conducted with other state-of-the-art area estimation algorithms.

The organization of this paper is in the following manner. The study area and dataset description are given in Section II. Section III presents the methodology and proposed adaptive linear mixture model for crop area estimation. Section IV presents the simulation results and accuracy assessments.

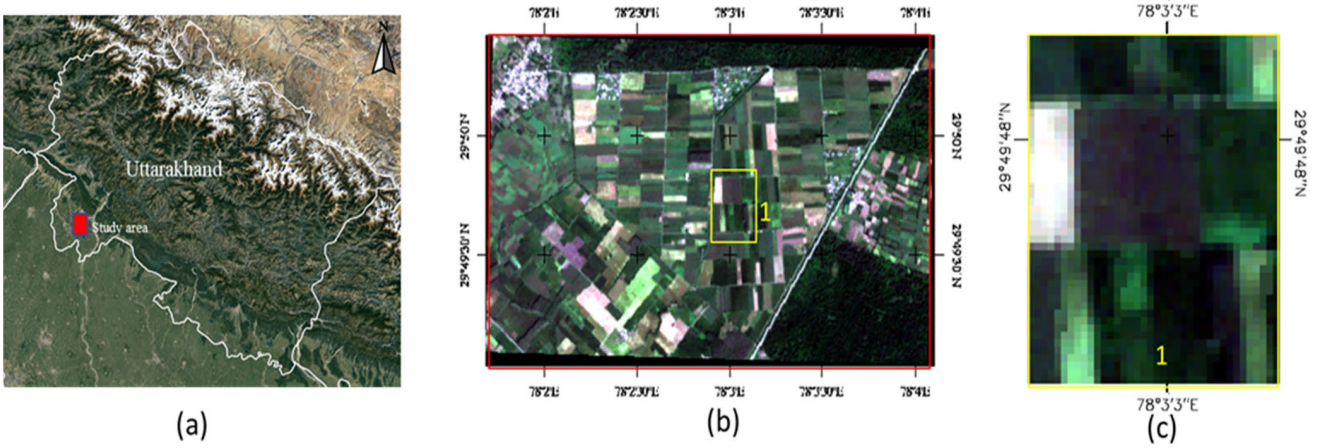

FIGURE 1. (a) Google earth imagery of study region, (b) Sentinel-2 imagery of agriculture field, and (c) subset of Sentinel-2 image of study area.

Finally, Section V conclude the paper and present future scope of the study.

II. STUDY AREA AND DATASET PREPARATION

In this section, we define our study area, dataset used for developing and validating the proposed algorithm.

A. STUDY AREA

The study area selected for experimentation is an agricultural farm land situated in Roorkee region of the Haridwar district in Uttarakhand state of India. This region predominantly contains small farm lands that are less than two hectares. The most agricultural task in this region is carried out in the monsoon season and winter season, which are most agricultural growing season of this area. The most prominent crops that are cultivated in Roorkee region is sugarcane and paddy which are grown in the monsoon season. The selected study area is shown in Fig. 1(a) with center latitude 78°3'3'' E and longitude 29°49'48'' N, mostly contains the bare soil, sugarcane and paddy land cover classes. For the experimentation purpose various field survey of study area is conducted to obtained the actual ground information that are utilize as knowledge base in addition of satellite image and drone image.

B. SATELLITE DATA USED AND PREPROCESSING

Satellite images were extracted from Sentinel-2 MSI dataset using a JavaScript written in Google Earth Engine's code editor. The script specified which image collection to be used, what date range to be used for image extraction, and how to export region-specified images to a google drive. For preparing images to be used for our study, the cloud and cirrus granules had to be removed to filter out the noise. This was consequently done by setting bit masks of cloud and cirrus to 0 and using a pre-filter in the image to set cloud pixel percentage to be 20%. This filter indicates that the map generated by adding layers should be clear, with little to no cloud granules to be present in the map generated. The study area mark in Fig. 1(b) is acquired from the sentinel data on October 7, 2018. This particular duration is chosen for this study because all the crop of winter season is grown in this duration which provide an equitably rich discrimination for classification of crop type. Images extracted from Earth Engine script were used as an input dataset for this study. These images were extracted in accordance with the crop classes used for this study, which were Bare Land, sugarcane, and paddy pixels were grouped into one image, with the dimensions of the image being 47 × 38, with a total of 1786 pixels with either being of bare land, sugarcane, and paddy. Since images are extracted from Sentinel-2 MSI image dataset, each pixel has more than 3 bands (due to the usage of multi-spectral image instruments being used). The images contain pixels having 12 bands, with each band displaying different information. 1st band represents Aerosols, 2nd, 3rd, and 4th band represent Blue, Green and Red spectrum bands respectively, 5th band represents Red edge 1 (Wavelength of approximately 703.9 nm), 6th band represents Red edge 2 (Wavelength of around 740.2 nm), 7th band represents Red edge 3 (around 782.5 nm), 8th band implies of Near Infrared values, 8Ath band represents Red edge 4 (wavelength of approximately 864.8 nm), 9th band represents Water Vapour values, 11th band represents Short Wave Infrared (SWIR 1) values wavelength of around 1613.7 nm and 12th band represents SWIR 2 values of wavelengths around 2202.4 nm. Images downloaded were of Tagged Image Format (.tif) format, hence they were read using GDAL library. The data read from images were in the form of a 3-D NumPy array, consisting of rows, columns and each pixel containing 12 values (from the 12 bands mentioned). The array was of the format M × N × 12 (Where M × N are total number of pixels and the 12 mentions the 12 bands worth of information present in that pixel). The Sentinel-2 image have spatial resolution of 10m to 60m and temporal resolution 5 days. Sentinel-2 image bands are resampled to particular spatial resolution of 10m based on nearest-neighbor resampling process using ESA's sentinel applications platform (SNAP). The resulting preprocessed Sentinel-2 image of desired study area where drone images are acquired is shown in Fig. 1(c).

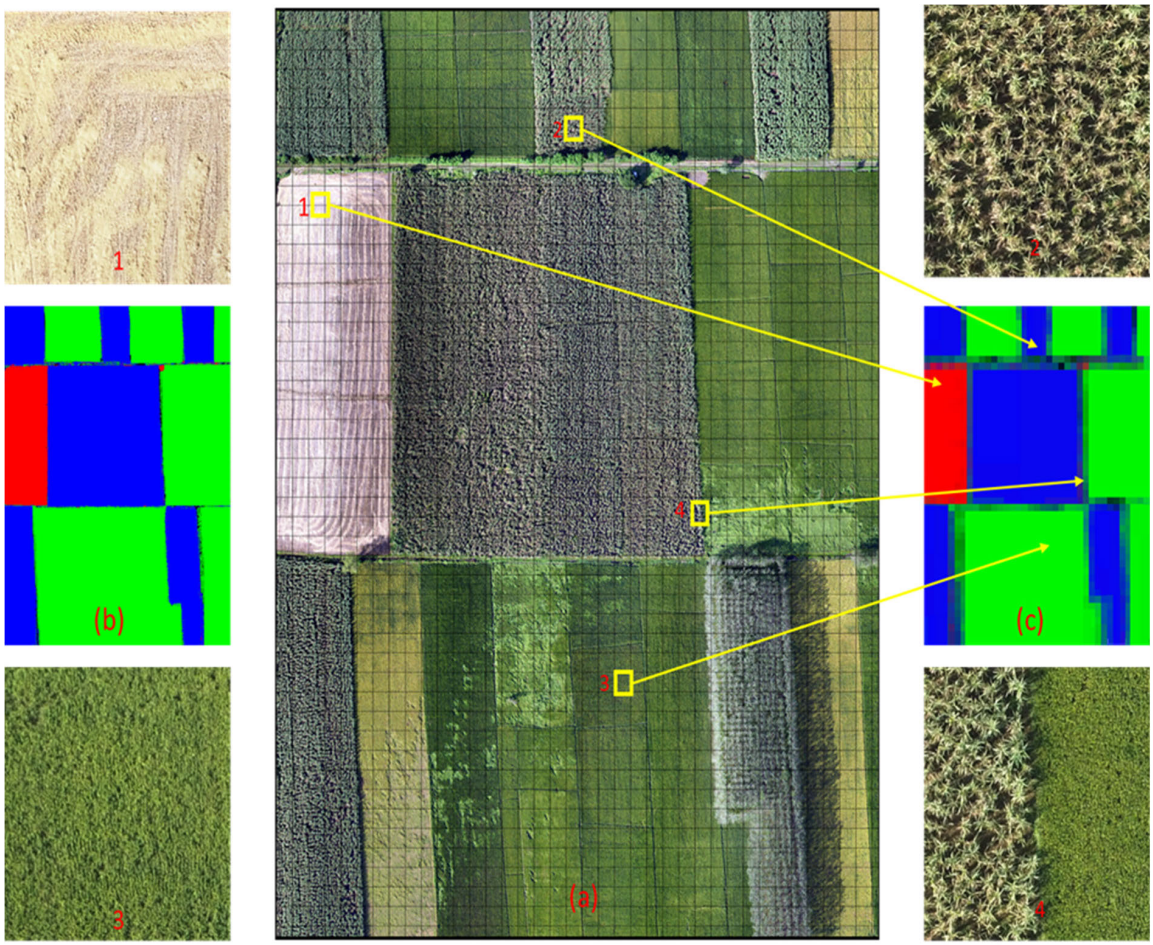

FIGURE 2. Ground truth data: (a) drone image with grids of 200 × 200 pixels with zoomed segments of pure and mixed pixels (1-4), (b) classified drone image of study area (bare soil (red), paddy(green), sugarcane(blue)), and (c) upscaled drone image to 10m spatial resolution.

C. GROUND TRUTH DATA PREPARATION

The reference data for ground truth is prepared using drone and GPS field survey on the same date of satellite passing from study area. The quadcopter DJI phantom 3 professional which have Sony 4K camera with 12.4-megapixel sensor is utilize as the image acquisition system. The quadcopter is operated at height of 120 m that acquire images with size of (4000 × 3000) pixels. The navigation path of the quadcopter drone is set such that it acquired images of study region with 65% forward overlap and 40% side overlap. This overlap of images provides good result in feature matching points while mosaicking the acquired images to obtained the high-resolution image of study area. The processing of the acquired drone images is done in lab using Pix4d software tool to obtain the single mosaic image of study area of size 9400 × 7600. The spatial resolution of the obtained mosaic image is 0.05m which is orthorectified and georeferenced that signifies that projection of every pixel is corrected and have location information of every pixel in the image. The acquired mosaic image is utilized for the ground truth data preparation. A gridding of 200 × 200 pixels is made over the drone image in order to make same area corresponding to each pixel of Sentinel-2 image as shown in Fig. 2 (a). Gridded segments of mosaic drone image contain bare soil, sugarcane, paddy and mixed classes which is lies in the particular grid area shown in the zoomed segment (1 - 4) in Fig. 2. The zoomed segment 1 to 3 are example of pure pixel class while 4 is of mixed class pixel. This high resolution mosaiced drone image is classified using maximum likelihood algorithm in various land cover classes shown in Fig. 2 (b). In order to make the reference of Sentinel-2 image, the classified drone image is upscale to the size of Sentinel-2 image pixel using pixel aggregate method as shown in Fig. 2 (c).

III. PROPOSED METHODOLOGY AND IMPLEMENTATION

Spectral and spatial information have been used to develop an adaptive linear mixture model for decomposition of mixed pixels to improve area estimation of land cover classes. The proposed methodology includes three major steps: classification of satellite images based on spectral values of pixels, mixed pixel extraction and decomposition using automatic endmembers selection in linear mixing model with the help of spatial information, and finally, area estimation and accuracy assessment is done using reference ground truth

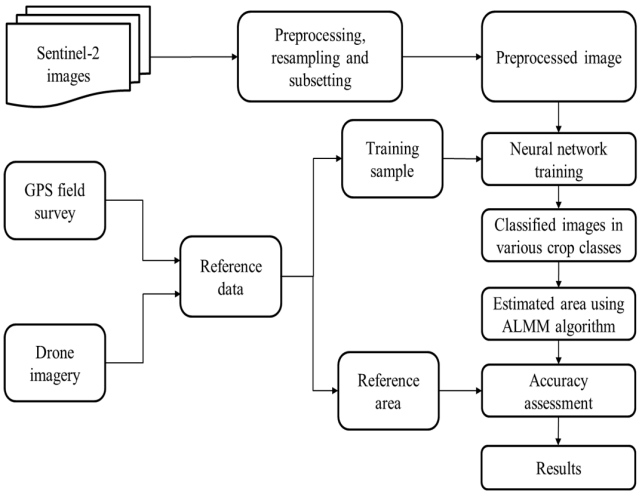

FIGURE 3. Flowchart of the proposed methodology.

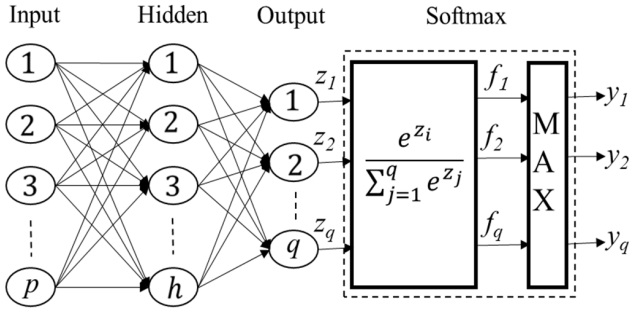

FIGURE 4. ANN model with one hidden layer and Softmax function [35].

data. The flowchart of proposed method of land cover area estimation is presented in Fig. 3.

A. CROP LAND CLASSIFICATION

An artificial neural network (ANN) is considered as a potential machine learning method to solve various real-world problems which are hard to solve using traditional programming. In wide range of network architecture, land cover classification can be achieved with multi-layer-feed-forward network. A network with one hidden layer is shown in Fig. 4. A multi-layer-feed-forward network is trained with reference dataset generated by GPS field surveys and high-resolution drone images using back-propagation algorithm. The back-propagation algorithm is generalization of gradient descent learning algorithm. On each iteration, the back-propagation algorithm recursively computes the error and modifies the network weights in order to minimize the error between actual outputs and network outputs. Once the network is trained, the weights of the network are stable and the network can be used to classify the input into various output classes. Let S **is** a multispectral satellite image of size $m \times n$ pixels with p features (bands). A multi-layered-feed-forward network is employed for the classification of these satellite image pixels in $k = 1, \ldots, q$ land cover classes using spectral features $l = 1, \ldots, p$. The output layer of multi-layered-feed-forward network produces $Z = (z_1, \ldots, z_q)$ non-normalized q real numbers. The exponential function σ is used to normalize Z into probability proportional $F = (f_1, \ldots, f_q)$ for q classes. The exponential function σ is formulated as

$$\sigma(z)_i = \frac{e^{z_i}}{\sum_{j=1}^{q} e^{z_j}}, \text{ for } i = 1, \ldots, q \text{ and } Z = z_1, \ldots, z_q \quad (1)$$

After applying exponential function σ, output $f = f_1, \ldots, f_q$ will be in the range of o to 1. This output vector f shows the membership of q classes into satellite image pixel $S(x, y)$. A max function is applied to assign a class$y = (y_1, \ldots, y_q)$ to each pixel $S(x, y)$ of satellite image based on their maximum membership in $F = (f_1, \ldots, f_q)$.

B. PROPOSED LINEAR MIXTURE MODEL

The linear mixture model aims to unmix the mixed pixels that arises when low-resolution satellite images are employed for mapping small agricultural crop fields. The basic assumption of the linear mixture model is that photon reaches the sensor, interacts with all endmembers of land cover classes and the received energy can be considered as a simple sum of the energies received from all endmembers [45]. Each endmember in the scene will contribute an amount to the received signal which are the characteristics of all endmembers of that scene and proportional to the area covered. The mathematical representation of linear mixture model can be expressed as

$$R_l = \sum_{k=1}^{q} f_k r_{lk} + e_l \quad (2)$$

where l represents the spectral bands range from 1 to p and k represent endmembers in the range from 1 to q. R_l represent the reflectance of a mixed pixel from band l that contains multiple endmembers.f_k represents the fraction of endmember k within a mixed pixel. r_{lk} represent the spectral signature of endmember k for band l. e_l represent the residual error in the linear mixture model.

The unconstrained, partial constraint and fully constraint are three methods applied to solve the linear equation problem. In unconstraint method, the values of fractions f_k of all endmembers in the mixed pixel are permitted to pick any values that are required to minimize the residual error e_l. In partial constraint method, sum of fractions f_k of all endmembers in the mixed pixel leads to one. These two methods are allowed to pick any positive or negative values of fractions f_k to solve the linear equations. However, in fully constraint method, the values of fractions f_k of all endmembers in the mixed pixel are in the range of zero to one and sum of all f_k must be one. The conditions of fully constraint method are shown in equation 3.

$$\sum_{k=1}^{q} f_k = 1 \text{ and } 0 \leq f_k \leq 1 \quad (3)$$

However, we can observe from equation (2) and (3) that there will be p linear equations for p spectral bands of satellite image and one sum of fractions f_k of all endmembers within

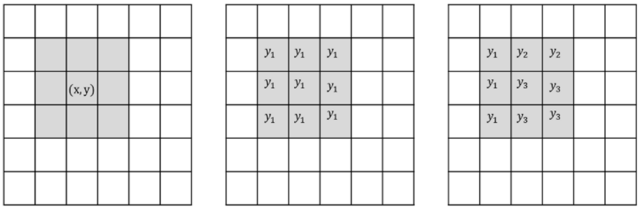

FIGURE 5. (a) $S'(x, y)$ and shaded spatially local pixels' area, (b) $S'(x, y)$ and local member in same class and (c) $S'(x, y)$ and local member in different classes.

a mixed pixel to one equation. From these $P + 1$ equations, we need to compute fraction f_k of q endmembers.

$$f_1 r_{11} + f_2 r_{12} + \ldots f_q r_{1q} = R_1 \quad (4)$$
$$f_1 r_{21} + f_2 r_{22} + \ldots f_q r_{2q} = R_2 \quad (5)$$
$$f_1 r_{p1} + f_2 r_{p2} + \ldots f_q r_{pq} = R_p \quad (6)$$
$$f_1 + f_2 + \ldots f_q = 1 \quad (7)$$

The theory of linear equation suggests that there will be a unique solution exist if $q = p+1$, and if $q < p + 1$ there will be no exact solution. Finally, when $q > p + 1$ there will an infinity of exact solutions and there is no clear way in which we should define any of exact solution. The important condition is $q \leq p+1$ that can give a solution for mixed pixel decomposition using least square error method.

$$f_k = \min_{f_k} \| r_{lk} f_k - R_l \|^2 \quad (8)$$

The success of linear mixture model is depending on the selections of endmembers. Therefore, we need to develop an approach for automatic endmember selection for linear mixture model.

1) SPATIALLY LOCAL MEMBERS

A spatially local member is a set of pixels in a certain window in a classified satellite image S'. In Fig. 5 (a), a pixel $S'(x, y)$ is shown in an arbitrary location of a classified satellite image S', and the small shaded region of 3×3 pixels is a local search window and points are spatially local member of $S'(x, y)$. This local search window shift pixel to pixel in the image to extract the pure pixel and mixed pixel endmembers of the image by applying bitwise logical operation on the classified masked image.

2) MIXED PIXEL AND PURE PIXEL EXTRACTION

In coarse spatial resolution satellite images, mixed pixels are the challenges for accurate land cover area estimation. To extract mixed pixel and pure pixel a specific local search window is used. This local search window is applied throughout the image and compute if all pixels within local search window belong to same land cover class, then central pixel is defined as a pure pixel, otherwise it is a mixed pixel. Let $y = (y_1, \ldots, y_q)$ be a set of q classes, k represents number of a class ($1 \leq k \leq q$) and y_k represents a pixel belongs to class k. Fig. 5 (a) shows the location of a pixel $S'(x, y)$ and shaded area shows the spatially local search window. Fig. 5 (b) and (c) show the classified pixels in classes y_k. In Fig. 5 (b) all the pixels are belongs to the same class that is y_1, so pixel $S'(x, y)$ count as pure pixel. In Fig. 5 (c) local members are belonging to different classes that is y_1, y_2 and y_3, so pixel $S'(x, y)$ count as mixed pixel. In order to identify these mixed pixel and pure pixel, we can use logical operators.

Logical 'OR' operation of localized pixels of $S'(x, y)$ in class k is defined as

$$C_k(x,y) = \vee_{i=x-1,j=y-1}^{i=x+1,j=y+1} S'(i,j) \quad (9)$$

$C_k(x,y)$ describe the existence of class k within localized pixels of *(x, y)*.

$$\begin{cases} C_k\,(x,y) = 1 & \textit{Class k is exist} \\ C_k\,(x,y) = 0 & \textit{Class is not exist} \end{cases} \quad (10)$$

Logical 'AND' operation of localized pixel of *(x, y)* in class k is defined as

$$D_k(x,y) = \wedge_{i=x-1,j=y-1}^{i=x+1,j=y+1} S'(i,j) \quad (11)$$

$D_k(x, y)$ describe the existence of pure and mixed pixel of class k at pixel *(x, y)*.

$$\begin{cases} D_k\,(x,y) = 1 \;\; \textit{Pixel}\;\; (x,y)\;\; \textit{is a pure pixel of class k} \\ D_k\,(x,y) = 0 \;\; \textit{Pixel}\;\; (x,y)\;\; \textit{is a mixed pixel of class k} \end{cases} \quad (12)$$

These logical operators are able to identify mixed pixel and pure pixel in the satellite images using spatial constraints.

Algorithm 1 ALMM (*S', E*)

Input: Satellite image S' and Endmember spectra E
Output: Area cover $A = (a_1, a_2, \ldots, a_q)$
Begin
Initialize a window of 3×3 pixels;
For $i \leftarrow 1$ *to* m
  For $j \leftarrow 1$ *to* n
    $\mathbf{E'} = \emptyset$
    For $k \leftarrow 1$ *to* q
      If $C_k\,(i,j) = 1$
        If $D_k\,(i,j) = 1$
          $a_k\,(i,j) = 1$;
        Else
          $E' \leftarrow E_k$;
      Else
        $a_k\,(i,j) = 0$;
    End
    $a_k\,(i,j) = \min_{f_k} \| r_{lk} f_k - R_l \|^2$ *where* $k \in E'$
  End
End
Return A;
End

3) ADAPTIVE LINEAR MIXTURE MODEL

In order to improve the accuracy of land cover area estimation, mixed pixels should be decomposed. A fully constraint linear mixture model may be used to decompose these mixed pixels. However, the performance of the linear mixture model is depending on the selection of appropriate endmembers. To overcome this problem, we can use logical operators to extract mixed pixels and their endmembers to unmix the mixed pixel using least square error solution in linear mixture model. Let S' is classified satellite image and E is a set of spectral signatures of q classes. Logical 'AND' operator and logical 'OR' operator is used to extract mixed pixels and their potential endmember spectra E' for decomposition of mixed pixels to improve accuracy of crop area cover of each class. The area covers $A = (a_1, a_2, \ldots, a_q)$ of q classes is computed using **Algorithm 1**.

C. AREA ESTIMATION AND ACCURACY ASSESSMENT

Area cover of various land cover classes are computed by ALMM algorithm. For estimation of area of class k, multiply area cover a_k of the class k with spatial resolution of the satellite image. The approximate area of various land cover classes is computed using Sentinel-2 image. The accuracy assessment of ALMM algorithm for land cover area estimation are done with the help of reference data, which are prepared with the help of drone and GPS field survey. For this purpose, drone was flown in study area and after preprocessing and mosaicking reference image was generated. This high-resolution drone image is classified and upscale to equivalent satellite image for pixel wise and class wise accuracy assessment of ALMM algorithm.

IV. RESULTS AND DISCUSSION

To evaluate the performance of various crop area estimation algorithms, a field experiment was conducted in agriculture field near Roorkee, Uttarakhand, India. The proposed ALMM algorithm and traditional ANN, fuzzy and ANF algorithm are applied to Sentinel-2 image of study area. A reference image of study area created by drone and GPS is used to evaluate the performance of traditional ANN, fuzzy, ANF and proposed ALMM algorithm. The experimental results of land cover area estimation of various land cover classes like bare soil, sugarcane and, paddy using ANN, fuzzy, ANF and ALMM algorithms are shown in Fig. 6. The color variation in the output image represents the membership of land cover classes, ranging from 0 to 1.

The accuracy assessment of mixed pixel and pure pixel extraction using proposed ALMM algorithm is illustrated by confusion matrix shown in Table 1. Sensitivity and specificity are two measure that are used to evaluating the performance of a classification algorithm when there are two classes. Sensitivity is defined as the number of positive pixels extracted out of total positive pixels in study area shown in (13). On the other hand, Specificity is the number of negative pixels extracted out of total negative pixels in study area shown in (14).

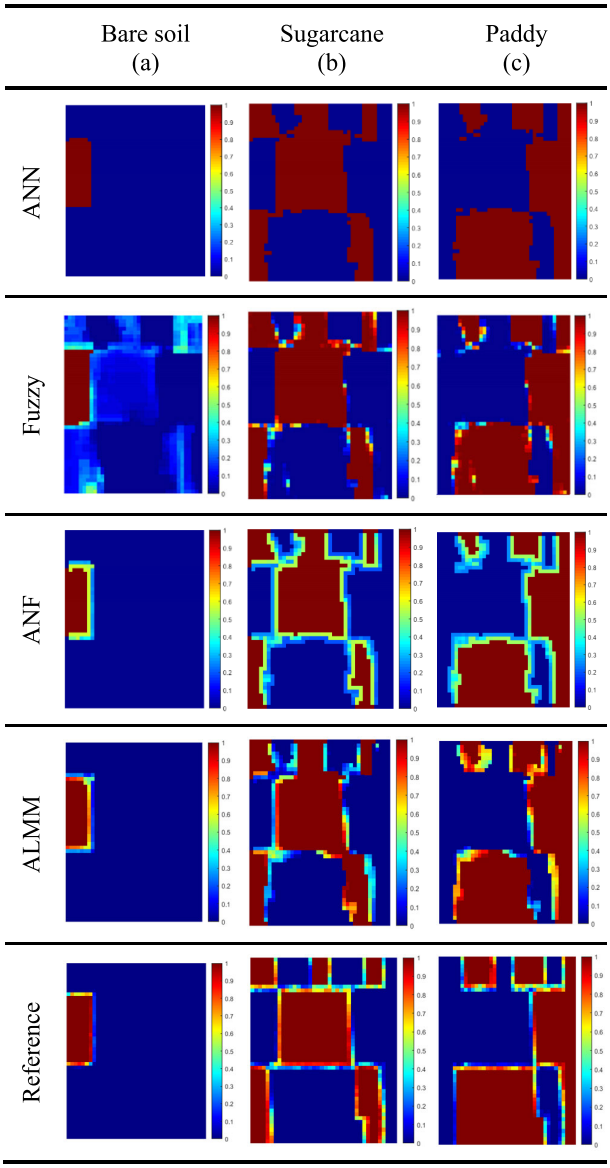

FIGURE 6. Land cover information of bare soil, sugarcane, and paddy in column (a), (b), and (c); Rows 1 to 5 represent the output results of ANN, fuzzy, ANF, ALMM, and reference image, respectively.

TABLE 1. Mixed pixel and pure pixel classification matrix.

		Reference Data		
		Pure	Mixed	Total
Classified Data	Pure	1344	0	1344
	Mixed	80	362	442
	Total	1424	362	1786

$$Sensitivity = \frac{TP}{TP + FN} \times 100\% \tag{13}$$

$$Specificity = \frac{TN}{TN + FP} \times 100\% \tag{14}$$

TABLE 2. Class wise estimated area of various land cover classes.

Class	Area Computed (in m^2)					Error (%)			
	ANN	Fuzzy	ANF	ALMM	Drone	ANN	Fuzzy	ANF	ALMM
Bare soil	13100	26661	14500	13476	13854	-5.44	+92.44	+4.66	-2.72
Sugarcane	76100	62792	74709	73586	71711	+6.12	-12.43	+4.18	+2.61
Paddy	89400	89147	89391	91538	93035	-3.90	-4.17	-3.91	-1.60

In case of mixed pixel and pure pixel classification algorithm true positive (TP) and true negative (TN) represents the proportion where mixed pixel classified as mixed pixel and pure pixel classified as pure pixel, respectively. Similarly, false positive (FP) and false negative (FN) represents the misclassification of algorithm identifying pure pixel as mixed pixel and mixed pixel as pure pixel, respectively. The accuracy of the area estimation for the land cover classes are improved by the proposed ALMM algorithm through decomposition of mixed pixels. For this purpose, high sensitivity is required in the classification of mixed pixels. It is depicted from the Table 1, the sensitivity for the mixed pixel classification is computed as $100\%\left(\frac{362}{362}\times 100\%\right)$ and the specificity is computed as $94.38\%\left(\frac{1344}{1424}\times 100\%\right)$.

Because the sub-pixel analysis algorithm outperformed pixel-based crop area estimation algorithm. Therefore, a comprehensive comparison at pixel level decomposition of mixed pixels were conducted between proposed ALMM algorithm and traditional ANF algorithm. To measure the performance of these algorithms, two common indicators, the root mean square error (RMSE) and the average difference (AD) were used. The RMSE measures the global error in the area estimation algorithm for land cover classes, whereas AD measures the bias of estimated area for land cover classes in the presented algorithms. These accuracy metrics were computed as follow:

$$RMSE = \sqrt{\frac{1}{N}\sum_{i=1}^{N}(\hat{f}_i - f_i)^2} \tag{15}$$

$$AD = \frac{1}{N}\sum_{i=1}^{N}\left(\hat{f}_i - f_i\right) \tag{16}$$

where, N referred to the number of mixed pixels. f_i is reference fractional area of land cover classes and $\hat{f}_i$ is estimated fractional area of land cover classes from area estimation algorithms for decomposition of mixed pixels.

Table 2 shows the mixed pixels decomposition results for the proposed ALMM algorithm and traditional ANF algorithm for various crop classes. The RMSE values of all crops reached from 0.07 to 0.09 in ALMM algorithm and 0.10 to 0.13 in ANF algorithm. However, all ADs are positive and negative values, which indicate that both the algorithms are constrained with abundance sum to one constraints and values are showing interclass biasness. From Table 3, we can see that RMSE and AD (bias) are reduced using the proposed ALMM algorithm compared to traditional ANF algorithm.

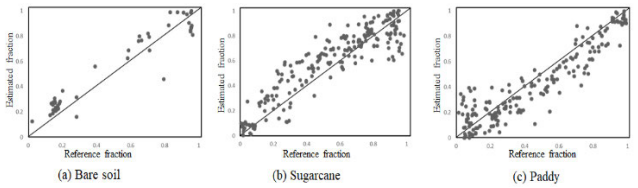

FIGURE 7. Scattered plot between reference and modelled fractions of (a) bare soil, (b) sugarcane and (c) paddy using ANF algorithm.

TABLE 3. Pixel wise accuracy assessment of ANF and ALMM algorithms.

Areas	ANF		ALMM	
	RMSE	AD (bias)	RMSE	AD (bias)
Bare soil	0.10	+0.04	0.07	-0.02
Sugarcane	0.13	+0.04	0.09	+0.02
Paddy	0.11	-0.03	0.07	-0.01

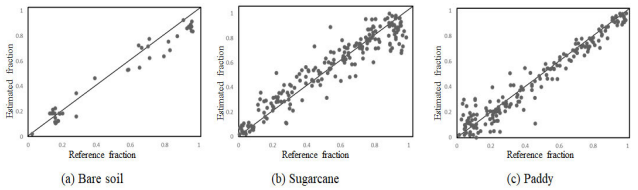

FIGURE 8. Scattered plot between reference and modelled fractions of (a) bare soil, (b) sugarcane and (c) paddy using ALMM algorithm.

Furthermore, scatter plots were drawn to demonstrate the association between the estimated area cover and reference area cover for various land cover classes in the mixed pixels. Fig. 7 and Fig. 8 illustrate that the proposed ALMM algorithm gives better results than traditional ANF algorithm. However, estimated crop area cover using proposed ALMM algorithm are closer to 1:1 line in scatter plots which exhibit the minimum RMSE and AD.

The class wise area estimation of various land cover classes such bare soil, sugarcane and paddy using traditional ANN, Fuzzy, ANF and proposed ALMM method are shown in Table 3. The error in estimated area of land cover classes using satellite images are calculated using ground truth information collected by drone and GPS field surveys. The error percentage of the computed area signifies that accuracy is improved using proposed ALMM algorithm over traditional ANN, Fuzzy and ANF methods. Further, the efficiency of the proposed ALMM algorithm is tested for the

multiple land cover classes in different satellite images and it found that it outperforms the traditional ANN, Fuzzy and ANF methods for finding the exact size of the land cover segments.

V. CONCLUSION AND FUTURE WORK

In the present study, an adaptive linear mixture model was proposed to improve the agriculture land cover area estimation using Sentinel-2 image. Sentinel-2 image was important for classifying land cover classes for the smallest parcel (100 m^2). The important advancement in this study was utilizing spectral and spatial information to extract optimal endmembers in linear mixture model. The neural network is employed for learning of spectral features of multispectral satellite images and classify each pixel into relevant land cover classes. The output of neural network was used as spatial constraints for mixed pixels extraction and decomposition using proposed adaptive linear mixture model to improve the accuracy of estimated crop area. Furthermore, our results suggest that our proposed algorithm can be used to accurately estimate the size of land cover classes. Finally, in future we call an extension for land cover pattern prediction of mixed classes in coarse resolution satellite images.

ACKNOWLEDGMENT

The authors would like to thank European Space Agency (ESA) for providing Sentinel-2 data.

REFERENCES

[1] N. Zhang, M. Wang, and N. Wang, "Precision agriculture—A worldwide overview," *Comput. Electron. Agricult.*, vol. 36, nos. 2–3, pp. 113–132, Nov. 2002.

[2] G. Azzari, M. J. David, and B. Lobell, "Towards fine resolution global maps of crop yields: Testing multiple methods and satellites in three countries," *Remote Sens. Environ.*, vol. 202, pp. 129–141, Dec. 2017.

[3] D. J. Mulla, "Twenty five years of remote sensing in precision agriculture: Key advances and remaining knowledge gaps," *Biosyst. Eng.*, vol. 114, no. 4, pp. 358–371, Apr. 2013.

[4] N. Wang, N. Zhang, and M. Wang, "Wireless sensors in agriculture and food industry-recent development and future perspective," *Comput. Electron. Agricult.*, vol. 50, no. 1, pp. 1–14, 2006.

[5] V. P. Kour and S. Arora, "Recent developments of the Internet of Things in agriculture: A survey," *IEEE Access*, vol. 8, pp. 129924–129957, 2020.

[6] A. K. Dwivedi, A. K. Singh, and D. Singh, "An object based image analysis of multispectral satellite and drone images for precision agriculture monitoring," in *Proc. IEEE Int. Geosci. Remote Sens. Symp.*, Jul. 2022, pp. 4899–4902.

[7] C. Zhang and J. M. Kovacs, "The application of small unmanned aerial systems for precision agriculture: A review," *Precis. Agricult.*, vol. 13, no. 6, pp. 693–712, Dec. 2012.

[8] K. Shaik, E. Prajwal, M. Bonu, and B. V. Reddy, "GPS based autonomous agricultural robot," in *Proc. Int. Conf. Design Innov. 3Cs Compute Communicate Control (ICDI3C)*, Apr. 2018, pp. 100–105.

[9] E. F. Abdelhafid, Y. M. Abdelkader, M. Ahmed, E. H. Doha, E. K. Oumayma, and E. A. Abdellah, "Localization based on DGPS for autonomous robots in precision agriculture," in *Proc. 2nd Int. Conf. Innov. Res. Appl. Sci., Eng. Technol. (IRASET)*, Mar. 2022, pp. 1–4.

[10] P. K. R. Maddikunta, S. Hakak, M. Alazab, S. Bhattacharya, T. R. Gadekallu, W. Z. Khan, and Q.-V. Pham, "Unmanned aerial vehicles in smart agriculture: Applications, requirements, and challenges," *IEEE Sensors J.*, vol. 21, no. 16, pp. 17608–17619, Aug. 2021.

[11] A. K. Singh, A. K. Dwivedi, M. Sumanth, and D. Singh, "An efficient approach for instance segmentation of railway track sleepers in low altitude UAV images using mask R-CNN," in *Proc. IEEE Int. Geosci. Remote Sens. Symp.*, Jul. 2022, pp. 4895–4898.

[12] J. Sridharani, S. Chowdary, and K. Nikhil, "Smart farming: The IoT based future agriculture," in *Proc. 4th Int. Conf. Smart Syst. Inventive Technol. (ICSSIT)*, Jan. 2022, pp. 150–155.

[13] P. Rao, W. Zhou, N. Bhattarai, A. K. Srivastava, B. Singh, S. Poonia, D. B. Lobell, and M. Jain, "Using Sentinel-1, Sentinel-2, and planet imagery to map crop type of smallholder farms," *Remote Sens.*, vol. 13, no. 10, p. 1870, May 2021.

[14] S. Condran, M. Bewong, M. Z. Islam, L. Maphosa, and L. Zheng, "Machine learning in precision agriculture: A survey on trends, applications and evaluations over two decades," *IEEE Access*, vol. 10, pp. 73786–73803, 2022.

[15] K. Rajamohan, "Image processing and artificial intelligence for precision agriculture," in *Proc. Int. Conf. Innov. Comput., Intell. Commun. Smart Electr. Syst. (ICSES)*, Jul. 2022, pp. 1–8.

[16] F. J. Gallego, "Remote sensing and land cover area estimation," *Int. J. Remote Sens.*, vol. 25, no. 15, pp. 3019–3047, Aug. 2004.

[17] A. Asgarian, A. Soffianian, and S. Pourmanafi, "Crop type mapping in a highly fragmented and heterogeneous agricultural landscape: A case of central Iran using multi-temporal Landsat 8 imagery," *Comput. Electron. Agricult.*, vol. 127, pp. 531–540, Sep. 2016.

[18] Q. Hu, D. Sulla-Menashe, B. Xu, H. Yin, H. Tang, P. Yang, and W. Wu, "A phenology-based spectral and temporal feature selection method for crop mapping from satellite time series," *Int. J. Appl. Earth Observ. Geoinf.*, vol. 80, pp. 218–229, Aug. 2019.

[19] X.-P. Song, P. V. Potapov, A. Krylov, L. King, C. M. Di Bella, A. Hudson, A. Khan, B. Adusei, S. V. Stehman, and M. C. Hansen, "National-scale soybean mapping and area estimation in the United States using medium resolution satellite imagery and field survey," *Remote Sens. Environ.*, vol. 190, pp. 383–395, Mar. 2017.

[20] P. Mishra and D. Singh, "A statistical-measure-based adaptive land cover classification algorithm by efficient utilization of polarimetric SAR observables," *IEEE Trans. Geosci. Remote Sens.*, vol. 52, no. 5, pp. 2889–2900, May 2014.

[21] A. Garg and D. Singh, "Development of an efficient contextual algorithm for discrimination of tall vegetation and urban for PALSAR data," *IEEE Trans. Geosci. Remote Sens.*, vol. 56, no. 6, pp. 3413–3420, Jun. 2018.

[22] D. Lu and Q. Weng, "A survey of image classification methods and techniques for improving classification performance," *Int. J. Remote Sens.*, vol. 28, no. 5, pp. 823–870, 2007.

[23] A. E. Maxwell, T. A. Warner, and F. Fang, "Implementation of machine-learning classification in remote sensing: An applied review," *Int. J. Remote Sens.*, vol. 39, no. 9, pp. 2784–2817, 2018.

[24] A. Agarwal, A. K. Singh, S. Kumar, and D. Singh, "Critical analysis of classification techniques for precision agriculture monitoring using satellite and drone," in *Proc. IEEE 13th Int. Conf. Ind. Inf. Syst. (ICIIS)*, Dec. 2018, pp. 83–88.

[25] J. M. Peña-Barragán, M. K. Ngugi, R. E. Plant, and J. Six, "Object-based crop identification using multiple vegetation indices, textural features and crop phenology," *Remote Sens. Environ.*, vol. 115, no. 6, pp. 1301–1316, Jun. 2011.

[26] N. R. Rao, P. K. Garg, and S. K. Ghosh, "Development of an agricultural crops spectral library and classification of crops at cultivar level using hyperspectral data," *Precis. Agricult.*, vol. 8, nos. 4–5, pp. 173–185, Nov. 2007.

[27] S. Huang and F. Siegert, "Land cover classification optimized to detect areas at risk of desertification in North China based on SPOT VEGETATION imagery," *J. Arid Environments*, vol. 67, no. 2, pp. 308–327, Oct. 2006.

[28] L. Ma, Y. Zhou, J. Chen, X. Cao, and X. Chen, "Estimation of fractional vegetation cover in semiarid areas by integrating endmember reflectance purification into nonlinear spectral mixture analysis," *IEEE Geosci. Remote Sens. Lett.*, vol. 12, no. 6, pp. 1175–1179, Jun. 2015.

[29] D. Murugan, A. Garg, T. Ahmed, and D. Singh, "Fusion of drone and satellite data for precision agriculture monitoring," in *Proc. 11th Int. Conf. Ind. Inf. Syst. (ICIIS)*, Dec. 2016, pp. 910–914.

[30] D. Murugan, A. Garg, and D. Singh, "Development of an adaptive approach for precision agriculture monitoring with drone and satellite data," *IEEE J. Sel. Topics Appl. Earth Observ. Remote Sens.*, vol. 10, no. 12, pp. 5322–5328, Dec. 2017.

[31] P. Fisher, "The pixel: A snare and a delusion," *Int. J. Remote Sens.*, vol. 18, no. 3, pp. 679–685, 1997.

[32] S. Fritz, L. See, I. McCallum, L. You, A. Bun, E. Moltchanova, and M. Duerauer, "Mapping global cropland and field size," *Global Change Biol.*, vol. 21, no. 5, pp. 1980–1992, 2015.
[33] A. Agarwal, S. Kumar, and D. Singh, "Development of neural network based adaptive change detection technique for land terrain monitoring with satellite and drone images," *Defence Sci. J.*, vol. 69, no. 5, pp. 474–480, Aug. 2019.
[34] A. K. Singh, A. K. Dwivedi, N. Nahar, and D. Singh, "Railway track sleeper detection in low altitude UAV imagery using deep convolutional neural network," in *Proc. IEEE Int. Geosci. Remote Sens. Symp.*, Jul. 2021, pp. 355–358.
[35] A. K. Dwivedi, S. Roy, and D. Singh, "An adaptive neuro-fuzzy approach for decomposition of mixed pixels to improve crop area estimation using satellite images," in *Proc. IEEE Int. Geosci. Remote Sens. Symp.*, Sep. 2020, pp. 4191–4194.
[36] N. A. Quarmby, J. R. G. Townshend, J. J. Settle, K. H. White, M. Milnes, T. L. Hindle, and N. Silleos, "Linear mixture modelling applied to AVHRR data for crop area estimation," *Int. J. Remote Sens.*, vol. 13, no. 3, pp. 415–425, Feb. 1992.
[37] P. E. Dennison and D. A. Roberts, "Endmember selection for multiple endmember spectral mixture analysis using endmember average RMSE," *Remote Sens. Environ.*, vol. 87, nos. 2–3, pp. 123–135, 2003.
[38] C. A. Bateson and B. Curtiss, "A method for manual endmember selection and spectral unmixing," *Remote Sens. Environ.*, vol. 55, no. 3, pp. 229–243, Mar. 1996.
[39] M. A. Theseira, G. Thomas, and C. A. D. Sannier, "An evaluation of spectral mixture modelling applied to a semi-arid environment," *Int. J. Remote Sens.*, vol. 23, no. 4, pp. 687–700, Jan. 2002.
[40] F. J. García-Haro, S. Sommer, and T. Kemper, "A new tool for variable multiple endmember spectral mixture analysis (VMESMA)," *Int. J. Remote Sens.*, vol. 26, no. 10, pp. 2135–2162, May 2005.
[41] B. Somers, G. P. Asner, L. Tits, and P. Coppin, "Endmember variability in spectral mixture analysis: A review," *Remote Sens. Environ.*, vol. 115, no. 7, pp. 1603–1616, 2011.
[42] A. Elmore, J. Mustard, S. Manning, and D. Lobell, "Quantifying vegetation change in semiarid environments: Precision and accuracy of spectral mixture analysis and the normalized difference vegetation index," *Remote Sens. Environ.*, vol. 73, pp. 87–102, Feb. 2000.
[43] J. Degerickx, D. A. Roberts, and B. Somers, "Enhancing the performance of multiple endmember spectral mixture analysis (MESMA) for urban land cover mapping using airborne LiDAR data and band selection," *Remote Sens. Environ.*, vol. 221, pp. 260–273, Feb. 2019.
[44] J. Franke, D. A. Roberts, K. Halligan, and G. Menz, "Hierarchical multiple endmember spectral mixture analysis (MESMA) of hyperspectral imagery for urban environments," *Remote Sens. Environ.*, vol. 113, no. 8, pp. 1712–1723, 2009.
[45] N. Keshava and J. F. Mustard, "Spectral unmixing," *IEEE signal Process. Mag.*, vol. 19, no. 1, pp. 44–57, Aug. 2002.

ARUN KANT DWIVEDI received the B.Tech. degree in computer science and engineering from Dr. A. P. J. Abdul Kalam Technical University (formerly, known as the Uttar Pradesh Technical University), in 2012, and the M.Tech. degree in computer science and engineering from the Indian Institute of Technology (Indian School of Mines) Dhanbad, Dhanbad, in 2015. He is currently pursuing the Ph.D. degree with the Department of computer science and engineering, Indian Institute of Technology Roorkee, Roorkee, Uttarakhand, India. His current research interests include satellite image processing, drone image processing, machine learning, and deep learning.

ARUN KUMAR SINGH (Member, IEEE) received the B.E. degree in computer science and engineering from ITM Gwalior, Madhya Pradesh, India, and the M.Tech. degree (Hons.) in information technology (IT) from the Madhav Institute of Technology and Sciences (MITS) Gwalior, Madhya Pradesh, India. He is currently pursuing the Ph.D. degree with the Department of Electronics and Communication Engineering, Indian Institute of Technology Roorkee, Roorkee, Uttarakhand, India. He also works in the projects sponsored by RailTel Corporation of India and ICAR India. His research interests include drone technology, computer vision, image processing, and deep learning.

DHARMENDRA SINGH (Senior Member, IEEE) received the Ph.D. degree in electronics engineering from Banaras Hindu University, Varanasi, India. He has more than 24 years of experience in teaching and research. He was a Visiting Scientist Postdoctoral Fellow with the Department of Information Engineering, Niigata University, Niigata, Japan; the German Aerospace Center, Cologne, Germany; the Institute for National Research in Informatics and Automobile, France; the Institute of Remote Sensing Applications, Beijing, China; Karlsruhe University, Karlsruhe, Germany; and the Polytechnic University of Catalonia, Barcelona, Spain. He also visited several other laboratories in other countries. He is currently a Professor with the Department of Electronics and Communication Engineering, Indian Institute of Technology Roorkee, Roorkee, India, and a Coordinator at the RailTel-IIT Roorkee Center of Excellence in Telecom, Roorkee. He has published more than 300 papers in various national/international journals and conferences. His research interests include microwave remote sensing, electromagnetic wave interaction with various media, polarimetric and interferometric applications of microwave data, and numerical modeling, ground penetrating radar, through wall imaging, and stealth technology. He has received various fellowships and awards from national and international bodies.

HARISH KUMAR received the Bachelor of Engineering degree in computer science and engineering from Visvesvaraya Technological University, India, the Master of Technology degree in computer cognition technology from Mysore University, India, and the Ph.D. degree in computer science and engineering from the Indian Institute of Technology Roorkee. He did his postdoctoral research at the INRIA Bordeaux Sud-Ouest, France. He has worked as the Chief Engineer at SEL, Samsung India Electronics Private Ltd., India. He is currently working as the University Professor with the Department of Computer Science, College of Computer Science, King Khalid University, Abha. He did his internship in the Samsung Global Internship Program 2008 at Samsung Electronics Company Ltd., Suwon, South Korea (he was one among two students from India, selected for the year 2008). He has several quality research papers in well-reputed journals. His research interests include augmented reality, virtual reality, security and privacy, HCI, steganography, machine learning, pattern recognition, natural language processing, computer vision, insider threats, fuzzy logic, deep learning, and soft computing. He has received the Young Scientist Award 2010 from the Second National Young Scientist Symposium 2010, Uttarakhand, India.